



1
2
3
4
5
6
7
8
9
10
11
12
13
14
15
16
17
18
19
20
21
22
23
24
25

University of Exeter's Institutional Repository, ORE

<https://ore.exeter.ac.uk/repository/>

Article version: POST-PRINT

Author(s): Michael N. Weiss, Daniel W. Franks, Kenneth C. Balcomb, David K. Ellifrit, Matthew J. Silk, Michael A. Cant, and Darren P. Croft

Article title: Modelling cetacean morbillivirus outbreaks in an endangered killer whale population

Originally published in: Biological Conservation

Link to published article (if available):

This is an Author's Original Manuscript of an article submitted for consideration in Biological Conservation.

Usage guidelines

Before reusing this item please check the rights under which it has been made available. Some items are restricted to non-commercial use. **Please cite the published version where applicable.**

Further information about usage policies can be found at:

<http://as.exeter.ac.uk/library/resources/openaccess/ore/orepolicies/>

26 **Modelling cetacean morbillivirus outbreaks in an endangered killer whale population**

27

28 Michael N. Weiss^{1,2*}, Daniel W. Franks³, Kenneth C. Balcomb², David K. Ellifrit², Matthew J. Silk⁴, Michael
29 A. Cant⁴, and Darren P. Croft¹

30 ¹ Centre for Research in Animal Behaviour, University of Exeter, Exeter, U.K. EX4 4QG

31 ² Center for Whale Research, Friday Harbor, WA, U.S.A. 98250

32 ³ Department of Biology and Department of Computer Science, University of York, York, U.K. YO10 5DD

33 ⁴ Centre for Ecology and Conservation, University of Exeter in Cornwall, Penryn, U.K. TR10 9FE

34

35 *Corresponding author

36 Email: mw607@exeter.ac.uk

37

38 **Acknowledgements**

39 We would like to thank all of the many volunteers and staff that have contributed to the field work for
40 Orca Survey that provided the photographs used in this study, as well the photographic ID catalogue for
41 this population. We'd also like to thank Emma Foster for her work developing the network construction
42 protocol used here.

43

44 **Role of funding source**

45 Data collection for this research was supported by funding from Earthwatch Institute and NOAA Fisheries.

46

47 **Declaration of Interest**

48 The authors declare they have no conflict of interest.

49

50 **Abstract**

51 The emergence of novel diseases represents a major hurdle for the recovery of endangered populations,
52 and in some cases may even present the threat of extinction. In recent years, epizootics of infectious
53 diseases have emerged as a major threat to marine mammal populations, particularly group-living
54 odontocetes. However, little research has explored the potential consequences of novel pathogens in
55 endangered cetacean populations. Here, we present the first study predicting the spread of infectious
56 disease over the social network of an entire free-ranging cetacean population, the southern resident killer
57 whale community (SRKW). Utilizing 5 years of detailed data on close contacts between individuals, we
58 build a fine-scale social network describing potential transmission pathways in this population. We then
59 simulate the spread of cetacean morbillivirus (CeMV) over this network. Our analysis suggests that the
60 SRKW population is highly vulnerable to CeMV. The majority of simulations resulted in unusual mortality
61 events (UMEs), with mortality rates predicted to be at least twice the recorded maximum annual
62 mortality. We find only limited evidence that this population's social structure inhibits disease spread.
63 Vaccination is not likely to be an efficient strategy for reducing the likelihood of UMEs, with over 40
64 vaccinated individuals (>50% of the population) required to reduce the likelihood of UMEs below 5%. This
65 analysis highlights the importance of modelling efforts in designing strategies to mitigate disease, and
66 suggests that populations with strong social preferences and distinct social units may still be highly
67 vulnerable to disease outbreaks.

68

69

70

71

72

73

74

75

76

77 **Keywords:** social network, epidemic modelling, *Orcinus orca*, SRKW, vaccination

78 Introduction

79 Infectious diseases, particularly novel pathogens emerging in naïve populations, can have severe
80 consequences for animal populations (Daszack *et al.* 2000). The consequences of these pathogens are
81 exacerbated in small, endangered populations, where disease can contribute to elevated extinction risk
82 (Pedersen *et al.* 2007). The prediction of infectious disease outbreaks through epidemic modelling, and
83 the subsequent design of mitigation strategies, is therefore a key task in endangered species
84 management. Traditional epidemic models assume that contact rates are homogenous within a
85 population (Allen 2008). However, this is rarely the case. In populations that are strongly spatially or
86 socially structured, these assumptions may hamper efforts to predict the severity and patterning of
87 disease outbreaks.

88 Network-based models have been increasingly used for analyzing disease dynamics in animal populations,
89 because they can incorporate spatial and social structure (Craft & Caillaud 2011; Godfrey 2013; Silk *et al.*
90 2017). In social network models, social entities (i.e. individuals or groups) are represented as nodes in a
91 graph, with the edges between nodes representing social connections and thus the opportunity for
92 disease transmission. A great deal of research has modelled disease outbreaks over the social networks
93 of terrestrial mammal populations, with the goals of predicting outbreak sizes, estimating temporal trends
94 in susceptibility, and designing vaccination strategies (e.g. chimpanzees (*Pan troglodytes*) and orangutans
95 (*Pongo pygmaeus*): Carne *et al.* 2014; raccoons (*Procyon lotor*): Reynolds *et al.* 2015; Japanese macaque
96 (*Macaca fuscata*): Romano *et al.* 2016; chimpanzees: Rushmore *et al.* 2014; African buffalo (*Syncerus*
97 *caffer*): Cross *et al.* 2004; Verreaux's sifakas (*Propithecus verreauxi*): Springer *et al.* 2017; European badgers
98 (*Meles meles*): Rozins & Silk *et al.* 2018). This work has highlighted the importance of considering non-
99 random social structures in wildlife epidemic modelling, and has suggested a role for social structure in
100 containing epidemics in natural populations.

101 Emergent infectious disease is of increasing concern for populations of cetaceans, many of which are
102 already threatened or endangered (Gulland & Hall 2007; Van Bresseem *et al.* 2009). Relatively little work,
103 however, has been done modelling the disease consequences of cetacean social structure. Guimares *et al.*
104 (2007) modelled the spread of a hypothetical pathogen in a subnetwork of mammal eating killer whales
105 (*Orcinus orca*), finding that the network was particularly vulnerable to disease outbreak. In this analysis,
106 the dynamics of the simulation were not tuned to any particular pathogen. More recently, unweighted
107 versions of networks derived from bottlenose dolphin populations (*Tursiops truncatus*) have been
108 analyzed as part of comparative and theoretical studies (Sah *et al.* 2017; Sah *et al.* 2018). Importantly, no

109 previous study has modelled the spread of specific pathogens over cetacean social networks with the goal
110 of predicting the severity of outbreaks, and none have modelled the spread through a complete
111 population.

112 Due to the logistical challenges of observing social interactions in wild cetaceans, the vast majority of
113 cetacean social network studies are based on association indices, which estimate the probability that
114 dyads associate in a given sampling period. Criteria for “association” are varied, but researchers typically
115 set a temporal or spatial threshold at which two individuals are considered to be together. A mismatch
116 between association criteria and disease transmission scales may have hampered previous
117 epidemiological studies; most cetacean social network studies that use a spatial threshold define
118 associations on broad scales, from 100 m (e.g. Lusseau *et al.* 2006) up to 10 km (e.g. Foster *et al.* 2012).
119 While these association criteria are often justified when trying to understand the patterns of social
120 relationships within a population, many pathogens of interest are typically transmitted over smaller
121 spatial scales, e.g. when animals exchange viruses through the respiratory tract. This mismatch between
122 contacts relevant to infection and network definitions may lead to incorrect inferences about the
123 dynamics of disease outbreaks (Craft 2015).

124 A pathogen of particular concern in gregarious cetacean species is cetacean morbillivirus (CeMV). CeMV
125 is an RNA virus belonging to the family *Paramyxoviridae*, which also contains measles virus, phocine
126 distemper virus, canine distemper virus, feline morbillivirus, and peste des petits ruminants virus (Alfonso
127 *et al.* 2016). CeMV is implicated as the cause of several unusual mortality events in wild cetaceans (Van
128 Bressems *et al.* 1999; Di Guardo *et al.* 2005). This virus is highly infectious, with high potential for
129 interspecies transmission (Jo *et al.* 2018) and is likely transmitted via the respiratory tract through the
130 inhalation of aerosolized virus (Van Bressems *et al.* 2014). Several factors may increase a population’s
131 susceptibility to CeMV, including high polychlorinated biphenyl (PCB) load (Aguilar & Borrell 1994), poor
132 nutrition (Aguilar & Raga 1993) and inbreeding (Valsecchi *et al.* 2003).

133 In this study, we use detailed social network data to model disease dynamics in an endangered killer whale
134 population, the southern resident killer whales (SRKW). The SRKW population is an extremely small (less
135 than 80 individuals), closed population of killer whales in the northeastern Pacific, frequenting the inland
136 waters of Washington and British Columbia. This population faces long-term threats from a variety of
137 environmental and anthropogenic factors. The three factors identified as primary hazards to this
138 population are the decline in abundance and quality of their primary prey, Chinook salmon (*Oncorhynchus*
139 *tshawytscha*), anthropogenic noise, and persistent organic pollutants (Lacy *et al.* 2017). In addition, recent

140 analysis of the respiratory microbiome of this population has highlighted pathogens as a potential fourth
141 threat (Raverty *et al.* 2017). Previous analysis has emphasized CeMV as a pathogen in need of further
142 study and monitoring in this population (Gaydos *et al.* 2004).

143 Killer whales are susceptible to CeMV infection; an Atlantic killer whale that stranded in 2002 was found
144 to be seropositive for CeMV antibodies, indicating recent exposure (Rowles *et al.* 2011). Morbillivirus
145 epizootics have not yet been recorded in any killer whale population and the virus has not been detected
146 in Pacific killer whales, but CeMV has high spillover potential from reservoirs into novel populations (Van
147 Bresse *et al.* 2014). SRKWs have been observed interacting with other cetacean species which are known
148 carriers of CeMV, including harbor porpoise (*Phocoena phocoena*), humpback whales (*Megaptera*
149 *novaengliae*), and Pacific white-sided dolphins (*Lagenorhynchus obliquidens*), providing a potential
150 pathway for the introduction of this pathogen into the population. In addition, many of the factors that
151 are thought to increase a population's susceptibility to CeMV are present in the SRKW community,
152 including high PCB load, inbreeding, and nutritional stress (Krahn *et al.* 2007; Ford *et al.* 2018; Ford *et al.*
153 2010).

154 The SRKW live in stable, multilevel social groups, and individuals form distinct social clusters (Bigg *et al.*
155 1990; Parsons *et al.* 2009; Ellis *et al.* 2017). The smallest, most stable social unit is the matriline, composed
156 of females and their descendants, which usually contain 2-9 whales. Closely related matriline form pods
157 that may contain over 40 individuals and exhibit distinct vocal dialects. The southern resident community
158 contains 3 pods, referred to as J, K, and L (Bigg *et al.* 1990). This social organization creates a modular
159 social network structure, although the implications of this multilevel social structure for disease
160 transmission in this population has yet to be established.

161 Modular networks have been hypothesized to provide fitness benefits to social species by trapping
162 disease within modules and preventing large-scale epidemics. Simulation studies predict that modular
163 contact networks result in smaller disease outbreaks than non-modular networks (Nunn *et al.* 2015; Sah
164 *et al.* 2017; Rozins & Silk *et al.* 2018). Recent comparative work has suggested that network subgrouping
165 may decrease outbreak size and epidemic probability, dependent on the characteristics of the disease and
166 strength of the subdivisions (Sah *et al.* 2018). An analysis of parasite load in primate social groups supports
167 the hypothesis that modular organization inhibits disease spread, with individuals in more modular groups
168 generally having lower parasite load (Griffin & Nunn 2012). In addition, the presence of pronounced social
169 preferences may itself aid in preventing disease spread. Strong social preferences result in increased
170 variance in edge weights (Whitehead 2008), and social networks with greater variance in edge weight are

171 predicted to generally experience smaller outbreaks of infectious disease (Yang & Zhou 2012; Wang *et al.*
172 2014). It is currently unclear if the modular structure and strong social preferences of the SRKW
173 community are capable of significantly reducing disease spread. Previous work in a closely related species
174 with a similar social structure, the long-finned pilot whale (*Globicephala melas*), demonstrated that
175 increased mortality after a CeMV epizootic was limited to a subset of social groups (Wierucka *et al.* 2014),
176 potentially indicating that modular social structures can effectively trap this disease.

177 Recently, there has been growing interest in applying individualized medical treatment to the SRKW
178 population (e.g. NOAA 2018), following the model of wildlife veterinary care that has been applied in
179 terrestrial systems such as mountain gorillas (Robbins *et al.* 2011). Such individualized care may include
180 prophylactic vaccination strategies. Although no morbillivirus vaccine is proven to be effective in any
181 cetacean species, a DNA vaccine for CeMV has been tested in bottlenose dolphins (Vaughan *et al.* 2007)
182 and recent genomic studies could further inform the development of new vaccines (Batley *et al.* 2018).
183 Logistical challenges and ethical considerations, however, may preclude vaccinations on a large scale in
184 wild populations. Nonetheless, network-based vaccination strategies to mitigate morbillivirus spread have
185 been successfully implemented in another endangered marine mammal, the Hawaiian monk seal
186 (*Monachus schauinslandi*; Robinson *et al.* 2018). Furthermore, herd immunity is thought to be more easily
187 induced in modular social networks, as individuals that bridge communities can be targeted for
188 vaccination, preventing global disease spread (Salathe & Jones 2010). It is currently unclear whether
189 vaccinating a realistic portion of the SRKW population would be effective at preventing epizootics.

190 Here, we use five years of detailed, fine-scale association data to inform a stochastic, network-based
191 model of pathogen spread through the SRKW population. We focus on simulating the epidemic
192 characteristics of cetacean morbillivirus based on previously published research, given its role in mass
193 mortality in other populations and the risk it poses to the SRKW. We further use null models of the social
194 network to determine the role that social structure has in shaping disease outbreaks. Finally, we simulate
195 both random and network-based vaccination strategies to determine if prophylactic treatment could
196 efficiently mitigate epizootics in this population.

197

198 **Methods**

199 *Field observations*

200 Social associations were recorded over five years (2011-2015) of opportunistic photographic identification
201 surveys in the inland waters of Washington and British Columbia conducted by the Center for Whale
202 Research (CWR). The purpose of these surveys was both to capture clear images of every whale present
203 during each encounter and to acquire photographs that could be used for assessment of body condition
204 and social affiliations. As the SRKW are protected by federal law in both the United States and Canada, all
205 field work was carried out under federal permits issued by both countries (NMFS 15569; DFO SARA 272).
206 Surfacing whales were photographed using Canon or Nikon DSLR cameras. Encounters only occurred on
207 days when clear photographic identification was possible (i.e. no rain and sea state less than Beaufort 4).
208 As the CWR has been conducting annual surveys of the SRKW population since 1976, all individuals in this
209 population are well known. Individuals are easily identifiable throughout their lives by unique
210 pigmentation patterns behind their dorsal fins (“saddle patches”), as well as by dorsal fin shape, knicks,
211 and scars they acquire throughout their lives (Bigg *et al.* 1990). Surveys were typically conducted from
212 small motorized vessels (5.5 m Boston Whaler), although shore-based photographs of sufficient quality to
213 identify individuals and associations were also analyzed. Only in-focus, clear photograph sequences in
214 which all individuals were identifiable were analyzed. Photographs were managed and analyzed using
215 ACDSsee Photo Studio.

216

217 *Social network construction*

218 As CeMV is thought to be contracted primarily through the inhalation of aerosolized virus, our contact
219 network was constructed to reflect close surface associations, with the goal of estimating the frequency
220 of “respiratory contact” between dyads. While much is still unknown about the transmission dynamics of
221 CeMV, including how long the virus remains infectious in the air after exhalation, we chose a restricted
222 association criteria to ensure that our estimates of disease spread were conservative. Therefore, we
223 considered individuals surfacing synchronously or successively within one body length to be in respiratory
224 contact. Synchronous and successive surfacings were recorded from photographic series capturing
225 surfacing sequences. A surfacing was considered successive or synchronous when an individual began
226 surfacing before the previous individual became completely submerged (Figure 1a).

227 Individuals and social groups within the SRKW population differ in their use of the study area, and were
228 not continuously followed. Therefore, we are unable to directly estimate the total number of contact
229 events between individuals. Instead, we estimate the probability that each dyad came into contact on a

230 given day. We estimated daily respiratory contact probabilities by calculating dyadic simple ratio indices
231 (SRI; Cairn & Schwager 1987):

$$232 \quad \text{SRI}_{ij} = \frac{X_{ij}}{D_{ij}} \quad (1)$$

233 where X_{ij} is the number of days in which individual i was photographed in respiratory contact with
234 individual j , and D_{ij} is the total number of days on which either i or j were photographed. SRI values
235 represent an estimated daily association probability, and thus range from 0 to 1, with zero indicating
236 individuals were never observed in respiratory contact, while 1 indicates individuals were observed in
237 respiratory contact on every day that either was observed. Many cetacean network studies use a half-
238 weight index (HWI) to correct for biases in data collection, namely that individuals are often more likely
239 to be seen apart than together. However, in line with our goal of being conservative in our estimates of
240 disease spread, we chose to use SRI, as a dyad's SRI value will always be less than or equal to the same
241 dyad's HWI value.

242 During surveys, the primary objective was to photograph all whales present, with secondary goals of
243 recording social groupings and assessing the health of individuals. Groups of whales could not be
244 continually followed for all hours of the day, and it was therefore not possible to quantify the amount of
245 time associated dyads spend together on a given day. Moreover, not all individuals could be
246 simultaneously monitored and surveys were likely to miss surface associations. Therefore, our SRI values
247 are prone to underestimating daily contact probabilities, which may lead to overly-conservative estimates
248 of disease outcomes.

249 We limit our dataset to sampling days occurring in the summer months (May to September) of each year.
250 This is the period in which the southern residents are most frequently in the study area as they follow
251 returning Chinook salmon runs, and therefore provides the most detailed data on association patterns.
252 While some aspects of SRKW social structure change over longer time-scales, relationships are
253 consistently structured by pod and matriline, and changes are not predictable (Parsons *et al.* 2009).
254 Therefore, we aggregate association data across the entire study period, as this aggregation allows for
255 more precise estimates of dyadic contact probabilities (Whitehead 2008). In order to avoid biases in
256 estimated contact probabilities due to the births and deaths of individuals, only individuals that were alive
257 for the entire study period were included in our analysis.

258 To confirm the suitability of this approach, we compared all pairs of networks derived from each year of
259 data collection by calculating the Spearman correlation coefficient between dyadic SRI values across the

260 two years, with Mantel tests with 1,000 permutations to assess statistical significance of the correlations
261 (Hobson *et al.* 2013). We also tested for seasonal changes within the summer months by constructing
262 aggregated networks for each study month (May-September) across all years and carrying out the same
263 comparison procedure described above.

264 While the aggregation of several years of data allows for more precise estimates of contact probabilities,
265 it also presents the potential for increasing the density (i.e. number of edges) in our simulated networks
266 relative to the empirical annual contact patterns. Overestimating the density of contact networks can lead
267 to overestimation of disease spread in epidemiological simulations (Risau-Gusman 2011). We carry out a
268 simulation study to confirm that simulations based on the aggregated network do not result in higher
269 density networks that would be expected for a single year of associations. For each year, we simulate
270 associations for each dyad from a binomial distribution, using the observed annual dyadic sampling effort
271 (D_{ij} in eq. 1) as the sample size and the aggregated SRI value as the probability of success. The expected
272 mean annual density is then calculated from these simulated networks. We carry out this procedure
273 10,000 times to build a distribution of mean densities for our simulations, which is then compared to the
274 mean density of the observed annual networks. If aggregation results in increased density, the observed
275 mean density would be significantly lower than the simulated mean densities.

276 SRI networks were constructed in R (R Core Team 2017) using the *asnipe* package (Farine 2018) and
277 custom code, and the *vegan* package was used to conduct Mantel tests (Oksanen *et al.* 2018).

278

279 *Network metrics*

280 To evaluate the precision of our social network, we estimated the correlation between our measured
281 association indices and the underlying association probabilities. We first calculate the coefficient of
282 variation (CV) of our observed SRI values, and then estimate the CV of the underlying association
283 probabilities (S) via maximum likelihood, assuming the underlying associations follow a beta distribution.
284 The ratio of S to the observed CV is an estimate of the portion of variance in SRI values that is accounted
285 for by the variance in association probabilities, rather than sampling variance, and therefore approximates
286 the correlation between true and observed association indices. Correlations greater than 0.4 are generally
287 considered to indicate useful representations of the underlying social structure (Whitehead 2008).
288 Parameter fitting was performed in R, using the VGAM package for beta-binomial likelihood calculation
289 (Yee 2018).

290 We measure the extent to which individuals formed subgroups by performing community detection on
291 the contact network. We use a walktrap community detection algorithm implemented in the igraph R
292 package to detect communities (Csardi & Nepusz 2006). The modularity of the community division found
293 by this algorithm is a network-level measure of how strongly individuals associate within rather than
294 across social clusters.

295

296 *Temporal independence of respiratory contacts*

297 A key assumption of our disease transmission model (see below) is that the probability of a dyad coming
298 into respiratory contact on a given day is constant, and therefore independent of contacts in previous
299 days. Biologically, this would indicate that contacts dissolve and reform within a single day according to
300 constant contact probabilities, leading to temporal independence of associations.

301 We test this assumption by calculating the lagged association rate (LAR) across several time-lags in our
302 dataset. The LAR at time-lag τ estimates the probability that a dyad associated in a given day will also be
303 associating τ days later. Most analyses of LAR analyze extremely large values of τ (i.e. over 1,000 days) in
304 order to investigate the long-term temporal structure of associations. However, as we are interested in
305 transmission dynamics over considerably shorter timescales (see below), we only investigate LARs for
306 values of τ from 1 to 20 days.

307 Whitehead (1995) suggests comparing LARs to null association rates that represent the expected patterns
308 if individuals associated randomly. As our model does not assume random mixing, but rather temporal
309 independence, we use an alternative null association rate that approximates the expected LAR if
310 associations dissolve and reform between each sampling period with a constant probability of association
311 for each dyad. Let a_{ij} be the probability of an association between individuals i and j in each sampling
312 period (approximated by SRI_{ij}). The probability that i and j associate twice in any two sampling periods,
313 given independence, is then a_{ij}^2 . The expected LAR across all time-lags under temporal independence
314 (LAR_{null}) is then:

$$315 \quad LAR_{null} = \frac{\sum_i \sum_j a_{ij}^2}{\sum_i \sum_j a_{ij}} \quad (2)$$

316 We calculated 95% confidence intervals for LARs at each τ using jackknife resampling (Whitehead 1995).
317 LAR_{null} represents our null hypothesis of temporal independence, and we rejected this null hypothesis at

318 a given τ if the 95% confidence interval of the LAR at τ did not include LAR_{null} . All temporal analyses were
319 performed using custom R code available in the supplementary material.

320

321 *Disease outbreak model*

322 We simulate the spread of CeMV using a stochastic individual-based susceptible-infected-removed (SIR)
323 model over the killer whale respiratory contact network. Note that in SIR models, there is no difference
324 between dead and recovered, immune individuals; they are removed from the population and cannot
325 become infected again or spread the pathogen to others. While this framework is potentially overly
326 simplistic for some pathogens, recovery from CeMV confers life-long immunity and the virus has no carrier
327 state, meeting the basic assumptions of an SIR model (Van Bresse *et al.* 2014).

328 The model simulates a situation in which an interaction with a CeMV infected individual of another species
329 (e.g. Pacific white-sided dolphin, humpback whale, harbor porpoise) leads to the introduction of the
330 disease to the SRKW population via a single seed individual. Interspecific interactions are rarely observed,
331 and therefore we assume no further interspecific transmission after the initial introduction. As CeMV has
332 not been detected in this population in over 40 years of observations, all non-infected individuals start as
333 susceptible. Each time-step in the model represents a single day. We therefore model the probability that
334 an infected individual j transmits the disease to a susceptible individual i at time t (λ_{tij}) as the joint
335 probability that i and j come into contact on that day and that a given contact effectively transmits the
336 disease. As the fine-scale transmission dynamics of CeMV have not been resolved, we make the
337 simplifying assumption that for each day a susceptible individual is exposed to an infected individual, there
338 is a constant probability of transmission. We further simplify the model by assuming that daily contacts
339 are independent of one another. We use our estimated SRI values to approximate daily contact
340 probabilities, and so

$$341 \quad \lambda_{tij} = \beta \cdot SRI_{ij} \cdot I_{tj} \quad (3)$$

342 where β is the transmission coefficient, representing the per-contact probability of transmission, and I_{tj}
343 is an indicator variable that takes the value of 1 if j is infected at time t , and 0 otherwise. The probability
344 that susceptible individual i will become infected during timestep t (T_{ti}) is then

$$345 \quad T_{ti} = 1 - \prod_j (1 - \lambda_{tij}) \quad (4)$$

346 The probability that individuals already infected at the beginning of timestep t will be removed by
347 timestep $t+1$ is denoted by α (mean infectious period = $1/\alpha$). Individuals that become infected during t
348 cannot infect others or be removed until timestep $t+1$. The model run is terminated when there are no
349 infected individuals left, or until the time limit is reached. We limit the number of daily time-steps to 150,
350 as our dataset represents association patterns during a five-month period of the year. We do not include
351 non-pathogen induced baseline mortality in the model, as mortality rates over a single 5-month period
352 would be too low to have a significant impact on model predictions. The disease simulation model was
353 coded in R and is available in the supplementary materials.

354

355 *Model parameters and output*

356 The outcome of our model is influenced by the removal probability α , and the transmission coefficient β .
357 We therefore sought to estimate values of these parameters that most closely resemble those of previous
358 CeMV outbreaks in wild odontocetes. In the absence of data on CeMV outbreaks in killer whale
359 populations, we estimate the likely range of epidemic parameters of CeMV from previously published
360 epidemic modelling and social network studies of western Atlantic bottlenose dolphins. We note that
361 CeMV strains vary in their epidemiology, and that there are likely differences in recovery rates and
362 infectiousness between host species (Jo *et al.* 2018). The derived parameter values should therefore be
363 viewed as rough estimates based on the best available knowledge.

364 Morris *et al.* (2015) estimated a reproductive ratio for CeMV (the average number of secondary cases
365 expected from a single infected individual, R) of 2.58 during the peak of an epidemic (95% CI = 2.08-3.17)
366 and a removal rate of 0.12 (95% CI = 0.1-0.14). While the overall rate at which infected individuals infect
367 others was estimated in this analysis, this study did not estimate a per-contact transmission probability.

368 To estimate the per-contact transmission probability of CeMV during this previously observed epidemic,
369 we use a social network study carried out by Titcomb *et al.* (2015) on a subpopulation of western Atlantic
370 bottlenose dolphins in the Indian River Lagoon to estimate the mean strength ($\langle s \rangle$) of association networks
371 in this population. This study is the only large-scale social network study we are aware of in this species
372 that uses the same daily sampling period as our analysis, and spatially overlaps the CeMV outbreak from
373 which the other epidemic parameters were derived. This study reports a mean weighted degree in the
374 dolphin social network of 1.88 (95% CI = 1.63-2.13). We note that this study defined associations over
375 broader spatial scales than our analysis (100 m) and HWI was used, rather than SRI. These factors are

376 likely to produce estimates of $\langle s \rangle$ larger than our methodology, potentially leading to an underestimation
377 of the transmission coefficient for CeMV and making our estimates of CeMV spread conservative.

378 For each set of simulations, we generate a set of α , $\langle s \rangle$, R_0 , and seed individuals via Latin hypercube
379 sampling using the “lhs” R package (Carnell 2019). This sampling technique allows for a more efficient
380 exploration of the entire parameter space than sampling each variable independently (Seaholm *et al.*
381 1988). Parameter values for α , $\langle s \rangle$, and R_0 were drawn from continuous uniform distributions with ranges
382 equal to their reported 95% confidence intervals, while the seed individual is drawn from a discrete uniform
383 distribution on $[1, N]$, where N is the total number of individuals in the network (Table 1). We then
384 calculate β for each parameter set using a simple estimate of the reproductive ratio for epidemics on
385 weighted graphs (Kamp *et al.* 2013):

$$386 \quad R_0 = \frac{\beta \langle s \rangle}{\alpha} \quad (5)$$

387 which can be re-arranged to

$$388 \quad \beta = \frac{R_0 \alpha}{\langle s \rangle} \quad (6)$$

389 Our baseline simulation to assess overall vulnerability of the network consisted of 100,000 model runs.
390 We evaluate the outcome of the model first by calculating the probability that an outbreak results in an
391 “unusual mortality event” (UME; Gulland & Hall 2007). We use a simple heuristic to define UMEs, and say
392 a UME has occurred when a simulation results in predicted mortality at least 2x higher than the highest
393 recorded annual mortality rate in this population, which was 8.24% in 2016. Therefore, our definition of
394 a simulated UME was a simulation in which at least 16.47% of the population is predicted to die. While
395 the mortality rate of CeMV infected cetaceans is not known, individuals infected with viruses of this family
396 tend to exhibit mortality rates of 70% - 80% (Diallo *et al.* 2007). We therefore assume that mortality rates
397 due to CeMV were 70% of the final outbreak size, and thus our threshold outbreak size for UMEs was
398 23.53% of the population infected. While we use this threshold in the rest of the text, our general results
399 were robust to alterations to this heuristic. We also calculated the mean and standard deviation of the
400 outbreak size (the proportion of the population infected) during runs in which UMEs occurred as a
401 measure of predicted UME severity.

402 We also conducted a sensitivity analysis to determine which of our two parameters, α and β , was most
403 influential on the outcome of our simulation. We did this by calculating partial Spearman rank correlation
404 coefficients for the final outbreak sizes of our 100,000 model runs and their respective values of these

405 two parameters (Wu *et al.* 2013). Higher absolute values of these coefficients indicate a greater amount
406 of variance in the outcome of the simulation being due to variance in the parameter of interest, controlling
407 for other parameters.

408

409 *Influence of social structure on disease outbreaks*

410 We next sought to determine the extent to which the structure of SRKW social relationships shapes
411 disease spread. We do this by performing simulations of disease outbreaks on two null models. The first
412 is a mean-field null model, in which all contact probabilities between individuals are set to the mean
413 contact probability in the observed network. This model simulates a population that associates entirely at
414 random, and is therefore equivalent to traditional epidemic models that assume random mixing. The
415 second null model is an edge randomization, in which observed edge weights are randomly shuffled
416 between dyads. This retains the heterogeneity of social preferences, but removes the higher-order
417 structure of the network. In both null models, the mean strength (i.e. an individual's average contacts per
418 time step) from the observed network is retained.

419 We carry out the same simulation procedure outlined above on the null-model networks, and examine
420 the influence of network structure on disease dynamics by comparing the UME probability and mean UME
421 size between the observed network and the two null models.

422

423 *Effectiveness of vaccination*

424 We next investigated whether a prophylactic vaccination strategy would be effective in this population.
425 We simulate the implementation of three potential vaccination strategies. The first is a random
426 vaccination, in which V randomly chosen individuals are set as removed prior to the start of the simulated
427 outbreak. The other two strategies are both based on individuals' centrality in the network. In many
428 networks, targeting vaccinations towards individuals with high weighted degree is the most effective
429 strategy to induce herd immunity (Rushmore *et al.* 2014), however in networks with community structure,
430 targeting high betweenness individuals that bridge communities is sometimes more effective (Salathe &
431 Jones 2010). We simulate scenarios in which individuals are targeted either based on their weighted
432 degree or weighted betweenness. In both scenarios, the V individuals with the highest centrality are set
433 as removed prior to the start of the simulation.

434 We evaluate vaccination effectiveness relative to a “conservative coverage threshold” (Rushmore *et al.*
435 2014). We therefore define an effective vaccination coverage when UMEs do not occur in 95% of
436 simulations. We simulate values of V from 1 to 50 (coverage of 1%-70%), with 50,000 simulations for each
437 value of V and each vaccination strategy. We stress that safely vaccinating 50 free-ranging killer whales is
438 most likely an unrealistic management goal, even if a safe and effective CeMV vaccine is developed for
439 this species. Nonetheless, we simulate these high values to better illustrate the degree to which
440 vaccination may be effective in this population.

441

442 **Results**

443 *Respiratory contact structure*

444 The final respiratory contact network contained a total of 72 individuals sighted over the course of 314
445 days of observation. All individuals were photographed on at least 30 different days throughout the study
446 period, with a median of 82 days per individual. Estimation of social differentiation and subsequent
447 comparison to the observed CV suggested a highly differentiated social structure and a good correlation
448 between our observed network and the true underlying association probabilities ($S = 1.50$, $r = 0.70$).

449 All pairs of yearly networks were significantly positively correlated (range of r values= 0.41-0.58, all $p <$
450 0.001), as were monthly networks (range of r values = 0.38-0.56, all $p < 0.001$). We therefore conclude
451 that there is no evidence for significant changes in the patterns of social relationships within the summer
452 months during our study period, nor was there evidence that social structure shifted significantly across
453 the 5 years of the study. The mean density of annual networks was not different from the expected density
454 given aggregated SRI values and sampling effort (Supp. Figure 1).

455 The aggregated SRKW respiratory contact network formed a single, highly connected component (Figure
456 1b). Over 70% of dyads had a non-zero contact probability during the study period. Non-zero edge weights
457 ranged from 0.005 to 0.62, with the mean contact probability over all dyads being 0.03 (median = 0.01,
458 IQR = 0.03).

459 In agreement with previous studies (Parsons *et al.* 2009; Ellis *et al.* 2017), the network was distinctly
460 modular ($Q = 0.52$) and was divided into six social clusters. All but one cluster contained members of a
461 single pod, the exception being J pod’s cluster, which contained individual L87, an adult male that has
462 frequently changed social affiliation since his mother’s death in 2005 and has travelled with J pod since

463 2010 (Center for Whale Research 2018). L pod showed the most significant sub-pod structure, with three
464 identified social clusters. In contrast, J pod formed a single, large cluster (Figure 1).

465 Analysis of lagged association rates showed that the temporal patterns of association in the observed data
466 are largely similar to the expected patterns under temporal independence, given the observed association
467 preferences. While the LAR is typically slightly above the expected LAR, jackknifed 95% confidence
468 intervals overlap LAR_{null} (Supp. Figure 2). We conclude that our model's assumption of temporal
469 independence is unlikely to significantly bias the results of our simulations.

470

471 *Simulated disease outbreaks*

472 As expected, the outcome of the baseline simulation showed distinct bimodality; the disease either failed
473 to spread far beyond the initially infected individual, or most of the population became infected (Figure
474 2). The network was extremely susceptible to simulated CeMV outbreaks. The majority of simulations
475 resulted in unusual mortality events (UME probability = 0.69). When UMEs occurred, the disease typically
476 infected around 90% of the population (mean UME size = 0.89, SD = 0.09).

477 Sensitivity analysis using partial correlation coefficients suggested that the outcome of our model was
478 more sensitive to variation in the per-contact transmission rate than the recovery rate. The partial rank
479 correlation between outbreak size and transmission rate was 0.33, while the correlation with removal
480 rate was -0.18. This is not surprising, as our values of the removal rate were based on the results of explicit
481 epidemic modelling, while our estimates of the transmission rate were derived from a combination of
482 previously reported epidemic parameters and social network metrics. The uncertainty in our estimates of
483 the transmission rate therefore incorporate the uncertainty in recovery rate, basic reproductive number,
484 and contact rates. While our range of recovery rates was 0.1 to 0.14, our final values of the transmission
485 rate ranged from 0.1 to 0.27. This result highlights the need for further studies into the transmission
486 dynamics of CeMV to inform modelling and management efforts. We note, however, that our estimates
487 for the per-contact transmission rate of CeMV are highly conservative compared to the known
488 transmission rates of other morbilliviruses (e.g. the 90% transmission rate found in measles; Hamborsky
489 *et al.* 2015).

490

491 *Influence of social structure on disease outbreaks*

492 Comparison of results of simulations on the observed network to the two null models revealed that the
493 structuring of contacts in the observed network provided limited protection from disease outbreaks
494 (Figure 2). While UME probability was larger in the null models, the changes in UME probability were small
495 (mean-field UME probability = 0.74; edge-randomized UME probability = 0.72). Similarly, the size of UMEs
496 was slightly larger in both null models (mean-field: mean = 0.95, SD = 0.05; edge-randomized: mean =
497 0.93, SD = 0.06). In terms of number of individuals infected during UMEs, these differences amount to an
498 average increase of 3 individuals in the edge-randomized model, and 5 individuals in the mean-field
499 model. While these results suggest that both the strength and patterning of social preferences may lead
500 to measurable reductions in epidemic probability and size, they also clearly demonstrate that these
501 effects are likely not significant from the perspective of conservation planning in this population.

502

503 *Effectiveness of vaccinations*

504 Our network measures used to design vaccination strategies, weighted degree and betweenness, were
505 not strongly correlated (Spearman's $r = 0.24$), indicating that there would be significant differences
506 between vaccination strategies based on these measures. Both targeted vaccination strategies performed
507 better than the random vaccination strategy at reducing the probability of outbreaks, and both targeted
508 strategies performed similarly to one another. However, the differences in conservative coverage
509 thresholds were modest. Given random vaccination, 45 individuals (62.5% coverage) were required to
510 reduce UME probability below 0.05, compared to 40 individuals (55.6% coverage) in the betweenness
511 strategy and 42 individuals (58.3% coverage) in the weighted degree strategy.

512

513 **Discussion**

514 In this study, we assessed the vulnerability of a critically endangered killer whale population to outbreaks
515 of an infectious disease that has previously been identified as a potential hazard. In our analysis, designed
516 to replicate the observed properties of cetacean morbillivirus, most simulations resulted in outbreaks that
517 would likely result in unusual mortality events, and in these cases nearly the entirety of the population
518 became infected. Our results further suggest that the social structure of this population offers only limited
519 protection from disease outbreaks, and that vaccination programmes, even with relatively high coverage
520 and ideal targeting of individuals, are unlikely to efficiently reduce the risk of outbreaks. Given its fragile
521 state, it is unlikely that this population would recover from the sudden increase in mortality that would

522 result from a majority of the population becoming infected with CeMV. While this model was specifically
523 parameterized to simulate the spread of CeMV, the general vulnerability suggested by this analysis is likely
524 to be applicable to other highly infectious pathogens that can be spread via aerosols.

525 Theoretical models and comparative studies suggest that subgrouping in social networks reduces the risk
526 of disease spread (Griffin & Nunn 2012; Sah et al. 2018). Our findings generally support this result, with
527 the important caveat that the protection provided seems unlikely to be significant in a conservation
528 context for this population. This agrees with recent simulation experiments suggesting that disease spread
529 is only significantly inhibited at extreme modularity values, and that network fragmentation may be more
530 important than modularity (Sah *et al.* 2017). We suggest that this lack of significant protection is due to
531 the sheer density of connections in the killer whale network; while there were clear preferences for
532 associating within clusters, associations across clusters were still common. In addition, modular structures
533 are predicted to be most effective at trapping disease with low transmissibility (Sah *et al.* 2018). Social
534 structure may therefore be less effective at trapping pathogens such as morbilliviruses, which are highly
535 transmissible.

536 Both the distribution of contact probabilities and the degree of subgrouping had small but measurable
537 effects on the outcomes of simulated epidemics. The effect of edge weight variance may partially be
538 driven by the density of non-zero edges, as all individuals had the opportunity to interact in the mean-
539 field model, while the edge-randomization maintained the portion of edges from the original network,
540 although overall interaction rates were the same between the two models. In most cases, both the portion
541 of non-zero edges and variance in edge weights are the result of social preferences in association networks
542 (Whitehead 2008). Therefore, our findings suggest that both the intensity of social preference and the
543 patterning of relationships may be determinants of disease spread on animal social networks. However,
544 our study also demonstrates that small populations with strong social preferences and clear divisions
545 between social units may still be highly vulnerable to the emergence of novel pathogens.

546 It is important to note that factors not included in the model, such as potential changes in social behavior
547 after infection (e.g. Lopes *et al.* 2016; Stroeymeyt *et al.* 2018), the duration of daily social contacts,
548 transitivity effects in the daily contacts, the potential for continued interspecies transmission, and
549 variation in epidemic parameters, are likely to influence the actual outcome of CeMV outbreaks in this
550 population. Our analysis draws particular attention to current uncertainty about the per-contact
551 transmission rate of CeMV. We suggest that future empirical work address these knowledge gaps to better
552 inform management efforts. Regardless, the results of our model are concerning, and suggest that the

553 possibility of widespread disease outbreaks and their potential impact on SRKW vital rates should be
554 accounted for in future population assessments.

555 Our results demonstrate that it is difficult to induce effective herd immunity in the SRKW population by
556 partial vaccination of the population, even when vaccinations are ideally targeted based on network
557 centrality. At least 40 vaccinations (> 50% of the network) were required to reduce UME probability below
558 0.05, even with network-informed vaccination strategies. Modularity in contact structures is thought to
559 generally make targeted vaccination more effective (Salathe & Jones 2010), however the multilevel nature
560 of resident killer whale society complicates this; since family groups typically move together, there are no
561 single individuals responsible for the majority of the spread between modules that can be targeted for
562 vaccination. The logistical challenges of vaccinating and monitoring individuals at sea and the potential
563 stress these activities may cause the animals likely make the prospect of wide-scale vaccinations
564 impractical, as well as potentially unethical.

565 As individualized treatment is unlikely to be efficient, we suggest that management of potential disease
566 outbreaks is likely best addressed by increasing the overall health of the population. Since the 1990s, the
567 SRKW population has declined from nearly one hundred individuals to 73 at the time of writing. The most
568 severe pressure contributing to this ongoing decline is reduced availability of prey (Lacy *et al.* 2017). As a
569 result of consistently low food availability, visibly poor body condition is widespread in this population
570 (Fearnbach *et al.* 2018), as is hormonal evidence of nutritional stress (Ayres *et al.* 2012). Poor nutrition
571 may increase this population's vulnerability to CeMV and other pathogens (Aguilar & Raga 1993). While
572 inbreeding and PCB concentration are also of concern due to their link to CeMV outbreaks (Aguilar &
573 Borrell 1994; Valsecchi *et al.* 2003), these hazards are less readily addressed by conservation efforts.
574 Therefore, in line with previous recommendations, we suggest that management actions designed to
575 increase the abundance of Chinook salmon available to the SRKW are critical to mitigating the potential
576 impact of epizootics in this population.

577 Our analysis highlights the importance of applying modelling techniques in conservation planning, while
578 also highlighting the limitations of targeted vaccination as a disease management strategy. As
579 conservation interventions are always limited by both resources (Bottrill *et al.* 2008) and potential
580 negative impacts on individual animals (e.g. Woodroffe 2001), maximizing the payoff of management
581 actions is crucial. Individualized medical interventions in general, and vaccinations in particular, are
582 increasingly central to a number of conservation efforts. Previous work has demonstrated that modelling
583 techniques can often inform low-impact, effective, and efficient vaccination programs in endangered

584 wildlife populations, particularly in primarily solitary species (Robinson *et al.* 2018) and in group-living
585 species with well-defined territories (Haydon *et al.* 2006). Our analysis suggests that such actions may be
586 less effective in highly social, group-living populations with frequent social contact between subgroups,
587 even when these groups are well defined. These social structures may also be generally vulnerable to
588 disease outbreaks, despite their apparent modularity. Such social structures are prevalent in several taxa
589 of conservation concern, including cetaceans, elephants, and primates (Grueter *et al.* 2012). We
590 recommend that similar simulation studies be implemented when evaluating infectious disease risk and
591 management strategies in these systems.

592

593 **References**

- 594 Aguilar, A., & Borrell, A. (1994). Abnormally high polychlorinated biphenyl levels in striped dolphins
595 (*Stenella coeruleoalba*) affected by the 1990-1992 Mediterranean epizootic. *The Science of the*
596 *Total Environment*, 154(2–3), 237–247. [https://doi.org/10.1016/0048-9697\(94\)90091-4](https://doi.org/10.1016/0048-9697(94)90091-4)
- 597 Aguilar, A., & Raga, J. A. (1993). The Striped Dolphin Epizootic in the Mediterranean Sea. *Ambio*, 22(8),
598 524–528. <https://doi.org/10.1111/1467-9752.12272>
- 599 Alfonso, C. L., Amarasinghe, G. K., Banyai, K., et al. (2016) Taxonomy of the order *Mononegavirales*:
600 update 2016. *Archives of Virology*, 161(8), 2351-2360. <https://doi.org/10.1007/s00705-016-2880-1>
- 601 Allen L. J. S. (2008). An Introduction to Stochastic Epidemic Models. In: *Mathematical Epidemiology.*
602 *Lecture Notes in Mathematics 1945.* Brauer F., van den Driessche, P. & Wu, J. (eds). Springer,
603 Berlin, Heidelberg.
- 604 Ayres, K. L., Booth, R. K., Hempelmann, J. A., Koski, K. L., Emmons, C. K., Baird, R. W., Balcomb-Bartok, K.,
605 Hansen, M. B., Ford, M. J., & Wasser, S. K. (2012). Distinguishing the impacts of inadequate prey
606 and vessel traffic on an endangered killer whale (*Orcinus orca*) population. *PLoS ONE*, 7(6).
607 <https://doi.org/10.1371/journal.pone.0036842>
- 608 Batley, K. C., Attard, C. R. M., Castillo, J. S., Zanardo, N., Kemper, C. M., Beheregaray, L. B., & Möller, L.
609 M. (2018). Genome-wide association study of an unusual dolphin mortality event reveals candidate

610 genes for susceptibility and resistance to cetacean morbillivirus, (August), 1–15.
611 <https://doi.org/10.1111/eva.12747>

612 Bigg, M. A., Olesiuk, P. F., Ellis, G. M., Ford, J. K. B., & Balcomb, K. C. (1990). Social organization and
613 genealogy of resident killer whales (*Orcinus orca*) in the coastal waters of British Columbia and
614 Washington State. In P. Hammond, S. Mizroch, & G. Donovan (Eds.), *Individual Recognition of*
615 *Cetaceans: Use of Photo-Identification and Other Techniques to Estimate Population Parameters*
616 (pp. 383–405).

617 Bukreyev, A., Calisher, C. H., Dolnik, O., Domier, L. L., Du, R., Collins, P. L., ... Kuhn, J. H. (2016). Taxonomy
618 of the order *Mononegavirales*: update 2016, 2351–2360. [https://doi.org/10.1007/s00705-016-](https://doi.org/10.1007/s00705-016-2880-1)
619 [2880-1](https://doi.org/10.1007/s00705-016-2880-1)

620 Cairns, S. J. & Schwager, S. J. (1987) A comparison of association indices. *Animal Behaviour* 35, 151-169

621 Carne, C., Semple, S., Morrogh-Bernard, H., Zuberbühler, K., & Lehmann, J. (2014). The risk of disease to
622 great apes: Simulating disease spread in orang-utan (*Pongo pygmaeus wurmbii*) and chimpanzee
623 (*Pan troglodytes schweinfurthii*) association networks. *PLoS ONE*, 9(4).
624 <https://doi.org/10.1371/journal.pone.0095039>

625 Carnell, R. (2019) lhs: Latin Hypercube Samples. R package version 1.0.1. [https://CRAN.R-](https://CRAN.R-project.org/package=lhs)
626 [project.org/package=lhs](https://CRAN.R-project.org/package=lhs)

627 Center for Whale Research (2018). *Southern Resident Killer Whale ID Guide*. Center for Whale Research,
628 Friday Harbor, WA, USA

629 Csardi, G., & Nepusz, T. (2006). The igraph software package for complex network research,
630 InterJournal, Complex Systems 1695. <http://igraph.org>

631 Craft, M. E., & Caillaud, D. (2011). Network models: An underused tool in wildlife epidemiology?
632 *Interdisciplinary Perspectives on Infectious Diseases*, 2011. <https://doi.org/10.1155/2011/676949>

633 Craft, M. E. (2015). Infectious disease transmission and contact networks in wildlife and livestock.
634 *Philosophical Transactions of the Royal Society B: Biological Sciences*, 370(1669), 20140107–
635 20140107. <https://doi.org/10.1098/rstb.2014.0107>

636 Cross, P. C., Lloyd-smith, J. O., Bowers, J. A., Hay, C. T., Getz, W. M., Annales, S., ... Getz, W. M. (2004).
637 Integrating association data and disease dynamics in a social ungulate : bovine tuberculosis in
638 African buffalo in Kruger National Park. *Finnish Zoological and Botanical Publishing Board*, 41(6),
639 879–892.

640 Daszak, P., Cunningham, A. A., & Hyatt, A. D. (2000) Emerging Infectious Diseases of Wildlife – Threats to
641 Biodiversity and Human Health. *Science*, 287(5452), 443-449.

642 Di Guardo, G., Marruchella, G., Agrimi, U., & Kennedy, S. (2005). Morbillivirus infections in aquatic
643 mammals: A brief overview. *Journal of Veterinary Medicine Series A: Physiology Pathology Clinical*
644 *Medicine*, 52(2), 88–93. <https://doi.org/10.1111/j.1439-0442.2005.00693.x>

645 Ellis, S., Franks, D. W., Giles, D., Balcomb, K. C., Weiss, M. N., Cant, M. A., Natrass, S., & Croft, D. P.
646 (2017). Mortality risk and social network position in resident killer whales: sex differences and the
647 importance of resource abundance. *Proceedings of the Royal Society B: Biological Sciences*,
648 284(1865).

649 Farine, D. R. (2018). asnipe: Animal Social Network Inference and Permutations for Ecologists. R package
650 version 1.1.8. <https://CRAN.R-project.org/package=asnipe>

651 Fearnbach, H., Durban, J., Ellifrit, D., & Balcomb, K. (2018). Using aerial photogrammetry to detect
652 changes in body condition of endangered southern resident killer whales. *Endangered Species*
653 *Research*, 35, 175–180. <https://doi.org/10.3354/esr00883>

654 Ford, J. K. B., Ellis, G. M., Olesiuk, P. F., & Balcomb, K. C. (2010). Linking killer whale survival and prey
655 abundance: food limitation in the oceans’ apex predator? *Biology Letters*, 6(1), 139–142.
656 <https://doi.org/10.1098/rsbl.2009.0468>

657 Ford, M. J., Parsons, K. M., Ward, E. J., Hempelmann, J. A., Emmons, C. K., Hanson, B. M., Balcomb, K. C.,
658 & Park, L. K. (2018). Inbreeding in an endangered killer whale population. *Animal Conservation*
659 21(5), 423-432. <https://doi.org/10.1111/acv.12413>

660 Foster, E. A., Franks, D. W., Morrell, L. J., Balcomb, K. C., Parsons, K. M., van Ginneken, A., & Croft, D. P.
661 (2012). Social network correlates of food availability in an endangered population of killer whales,
662 *Orcinus orca*. *Animal Behaviour*, *83*, 731–736. <https://doi.org/10.1016/j.anbehav.2011.12.021>

663 Gaydos, J. K., Balcomb, K. C., Osborne, R. W., & Dierauf, L. (2004). Evaluating potential infectious disease
664 threats for southern resident killer whales, *Orcinus orca*: A model for endangered species.
665 *Biological Conservation*, *117*(3), 253–262. <https://doi.org/10.1016/j.biocon.2003.07.004>

666 Godfrey, S. S. (2013). Networks and the ecology of parasite transmission: A framework for wildlife
667 parasitology. *International Journal for Parasitology: Parasites and Wildlife*, *2*(1), 235–245.
668 <https://doi.org/10.1016/j.ijppaw.2013.09.001>

669 Griffin, R. H., & Nunn, C. L. (2012). Community structure and the spread of infectious disease in primate
670 social networks. *Evolutionary Ecology*, *26*(4), 779–800. <https://doi.org/10.1007/s10682-011-9526-2>

671 Grueter, C. C., Matsuda, I., Zhang, P., and Zinner, D. (2012) Multilevel societies in primates and other
672 mammals: Introduction to the special issue. *International Journal of Primatology*, *33*(5), 993-1001.
673 [10.1007/s10764-012-9614-3](https://doi.org/10.1007/s10764-012-9614-3)

674 Guimarães, P. R., De Menezes, M. A., Baird, R. W., Lusseau, D., Guimarães, P., & Dos Reis, S. F. (2007).
675 Vulnerability of a killer whale social network to disease outbreaks. *Physical Review E - Statistical,*
676 *Nonlinear, and Soft Matter Physics*, *76*(4), 42901. <https://doi.org/10.1103/PhysRevE.76.042901>

677 Gulland, F. M. D., & Hall, A. J. (2007). Is Marine Mammal Health Deteriorating? Trends in the Global
678 Reporting of Marine Mammal Disease. *EcoHealth*, *4*(2), 135–150. [https://doi.org/10.1007/s10393-](https://doi.org/10.1007/s10393-007-0097-1)
679 [007-0097-1](https://doi.org/10.1007/s10393-007-0097-1)

680 Hamborsky, J., Kroger, A., & Wolfe, C. (2015). Epidemiology and prevention of vaccine-preventable
681 diseases. United States: U.S. Dept. of Health & Human Services, Centers for Disease Control and
682 Prevention.

683 Haydon, D. T., Randall, D. A., Matthews, L., Knobel, D. L., Tallents, L. A., Gravenor, M. B., Williams, S. D.,
684 Pollinger, J. P., Cleaveland, S., Woolhouse, M. E. J., Sillero-Zubiri, C., Marino, J., Macdonald, D. W.,
685 & Laurenson, M. K. (2006). Low-coverage vaccination strategies for the conservation of
686 endangered species. *Nature*, *443*, 692-695. <https://doi.org/10.1038/nature05177>

687 Hobson, E. A., Avery, M. L., & Wright, T. F. (2013). An analytical framework for quantifying and testing
688 patterns of temporal dynamics in social networks. *Animal Behaviour*, 85(1), 83-96.
689 <https://doi.org/10.1016/j.anbehav.2012.10.010>

690 Jo, W. K., Osterhaus, A. D. M. E., & Ludlow, M. (n.d.). ScienceDirect Transmission of morbilliviruses
691 within and among marine mammal species. *Current Opinion in Virology*, 28, 133–141.
692 <https://doi.org/10.1016/j.coviro.2017.12.005>

693 Kamp, C., Moslonka-Lefebvre, M., & Alizon, S. (2013). Epidemic Spread on Weighted Networks. *PLoS*
694 *Computational Biology*, 9(12). <https://doi.org/10.1371/journal.pcbi.1003352>

695 Krahn, M. M., Hanson, M. B., Baird, R. W., Boyer, R. H., Burrows, D. G., Emmons, C. K., Ford, J. K. B.,
696 Jones, L. L., Noren, D. P., Ross, P. S., Schorr, G. S., & Collier, T. K. (2007). Persistent organic
697 pollutants and stable isotopes in biopsy samples (2004/2006) from Southern Resident killer whales.
698 *Marine Pollution Bulletin*, 54(12), 1903–1911. <https://doi.org/10.1016/j.marpolbul.2007.08.015>

699 Krahn, M. M., Bradley Hanson, M., Schorr, G. S., Emmons, C. K., Burrows, D. G., Bolton, J. L., Baird, R. W.,
700 & Ylitalo, G. M. (2009). Effects of age, sex and reproductive status on persistent organic pollutant
701 concentrations in “Southern Resident” killer whales. *Marine Pollution Bulletin*, 58(10), 1522–1529.
702 <https://doi.org/10.1016/j.marpolbul.2009.05.014>

703 Lacy, R. C., Williams, R., Ashe, E., Balcomb, K. C., Brent, L. J. N., Clark, C. W., Croft, D. P., Giles, D. A.,
704 MacDuffee, M., & Paquet, P. C. (2017). Evaluating anthropogenic threats to endangered killer
705 whales to inform effective recovery plans. *Scientific Reports*, 7(1), 1–12.
706 <https://doi.org/10.1038/s41598-017-14471-0>

707 Lopes, P. C., Block, P. B., & Konig, B. (2016). Infection-induced behavioural changes reduce connectivity
708 and the potential for disease spread in wild mice contact networks. *Scientific Reports*, 6(1). 1-10.

709 Lusseau, D., Wilson, B., Hammond, P. S., Grellier, K., Durban, J. W., Parsons, K. M., Barton, T. R., &
710 Thompson, P. M. (2006). Quantifying the influence of sociality on population structure in
711 bottlenose dolphins. *Journal of Animal Ecology*, 75(1), 14–24. [https://doi.org/10.1111/j.1365-](https://doi.org/10.1111/j.1365-2656.2005.01013.x)
712 [2656.2005.01013.x](https://doi.org/10.1111/j.1365-2656.2005.01013.x)

713 Lusseau, D., Whitehead, H., & Gero, S. (2008). Incorporating uncertainty into the study of animal social
714 networks. *Animal Behaviour*, 75(5), 1809–1815. <https://doi.org/10.1016/j.anbehav.2007.10.029>

715 Morris, S. E., Zelner, J. L., Fauquier, D. A., Rowles, T. K., Rosel, P. E., Gulland, F., & Grenfell, B. T. (2015).
716 Partially observed epidemics in wildlife hosts: Modelling an outbreak of dolphin morbillivirus in the
717 northwestern Atlantic, June 2013-2014. *Journal of the Royal Society Interface*, 12(112), DOI:
718 10.1098/rsif.2015.0676. <https://doi.org/10.1098/rsif.2015.0676>

719 NOAA (2018), *Updates on Southern Resident Killer Whales J50 and J35*. Retrieved from:
720 [https://www.westcoast.fisheries.noaa.gov/protected_species/marine_mammals/killer_whale/upd](https://www.westcoast.fisheries.noaa.gov/protected_species/marine_mammals/killer_whale/updates-j50-j35.html)
721 [ates-j50-j35.html](https://www.westcoast.fisheries.noaa.gov/protected_species/marine_mammals/killer_whale/updates-j50-j35.html)

722 Nunn, C. L., Jordan, F., Mc-Cabe, C. M., Verdolin, J. L., & Fewell, J. H. (2015). Infectious disease and group
723 size: More than just a numbers game. *Philosophical Transactions of the Royal Society B: Biological*
724 *Sciences*, 370. <https://doi.org/10.1098/rstb.2014.0111>

725 Oksanen, J., Blanchet, F. G., Friendly, M., Kindt, R., Legendre, P., McGlenn, D., Minchin, P. R., O'Hara, R.
726 B., Simpson, G. L., Solymos, P., Stevens, M. H. H., Szoecs, E., & Wagner, H. (2018). vegan:
727 Community Ecology Package. R package version 2.4-6. <https://CRAN.R-project.org/package=vegan>

728 Parsons, K. M., Balcomb, K. C., Ford, J. K. B., & Durban, J. W. (2009). The social dynamics of southern
729 resident killer whales and conservation implications for this endangered population. *Animal*
730 *Behaviour*, 77(4), 963–971. <https://doi.org/10.1016/j.anbehav.2009.01.018>

731 Pedersen, A. B., Jones, K. E., Nunn, C. L., & Altizer, S. (2007). Infectious Diseases and Extinction Risk in
732 Wild Mammals. *Conservation Biology*, 21(5), 1269-1279.

733 R Core Team (2017). R: A language and environment for statistical computing. R Foundation for
734 Statistical Computing, Vienna, Austria. URL <https://www.R-project.org/>

735 Raverty, S. A., Rhodes, L. D., Zabek, E., Eshghi, A., Cameron, C. E., Hanson, M. B., & Schroeder, J. P.
736 (2017). Respiratory Microbiome of Endangered Southern Resident Killer Whales and Microbiota of
737 Surrounding Sea Surface Microlayer in the Eastern North Pacific. *Scientific Reports*, 7(1), 1–12.
738 <https://doi.org/10.1038/s41598-017-00457-5>

- 739 Reynolds, J. J. H., Hirsch, B. T., Gehrt, S. D., & Craft, M. E. (2015). Raccoon contact networks predict
740 seasonal susceptibility to rabies outbreaks and limitations of vaccination. *Journal of Animal*
741 *Ecology*, 84(6), 1720–1731. <https://doi.org/10.1111/1365-2656.12422>
- 742 Risau-Gusman, S. (2011) Influence of network dynamics on the spread of sexually transmitted diseases.
743 *Journal of the Royal Society Interface*, 9. <http://doi.org/10.1098/rsif.2011.0445>
- 744 Robbins M. M., Gray M., Fawcett K. A., Nutter F. B., Uwingeli P., Mburanumwe, I., Kagoda, E., Basobose,
745 A., Stoinski, T. S., Cranfield, M. R., Byamukama, J., Spelman, L. H., Robbins, A. M. (2011) Extreme
746 Conservation Leads to Recovery of the Virunga Mountain Gorillas. *PLOS ONE* 6(6).
747 e19788. <https://doi.org/10.1371/journal.pone.0019788>
- 748 Robinson, S. J., Barbieri, M. M., Murphy, S., Baker, J. D., Harting, A. L., Craft, M. E., & Littnan, C. L. (2018).
749 Model recommendations meet management reality: Implementation and evaluation of a network-
750 informed vaccination effort for endangered Hawaiian monk seals. *Proceedings of the Royal Society*
751 *B: Biological Sciences*, 285(1870). <https://doi.org/10.1098/rspb.2017.1899>
- 752 Romano, V., Duboscq, J., Sarabian, C., Thomas, E., Sueur, C., & MacIntosh, A. J. J. (2016). Modeling
753 infection transmission in primate networks to predict centrality-based risk. *American Journal of*
754 *Primatology*, 78(7), 767–779. <https://doi.org/10.1002/ajp.22542>
- 755 Rowles, T. K., Schwacke, L. S., Wells, R. S., Saliki, J. T., & Hansen, L. (2011). Evidence of susceptibility to
756 morbillivirus infection in cetaceans from the United States. *Marine Mammal Science*, 27(1), 1–19.
757 <https://doi.org/10.1111/j.1748-7692.2010.00393.x>
- 758 Rozins, C., Silk, M. J., Croft, D. P., Delahay, R. J., Hodgson, D. J., McDonald, R. A., Weber, N., & Boots, M.
759 (2018). Social structure contains epidemics and regulates individual roles in disease transmission in
760 a group living mammal. *Ecology and Evolution*, in press. <https://doi.org/10.1002/ece3.4664>
- 761 Rushmore, J., Caillaud, D., Hall, R. J., Stumpf, R. M., Meyers, L. A., & Altizer, S. (2014). Network-based
762 vaccination improves prospects for disease control in wild chimpanzees. *Journal of the Royal*
763 *Society Interface*, 11. <https://doi.org/http://dx.doi.org/10.1098/rsif.2014.0349>

- 764 Sah, P., Leu, S. T., Cross, P. C., Hudson, P. J., & Bansal, S. (2017). Unraveling the disease consequences
765 and mechanisms of modular structure in animal social networks. *Proceedings of the National*
766 *Academy of Sciences*, 114(16), 4165–4170. <https://doi.org/10.1073/pnas.1613616114>
- 767 Sah, P., Mann, J., & Bansal, S. (2018). Disease implications of animal social network structure: A
768 synthesis across social systems. *Journal of Animal Ecology*, 87(3), 546–558.
769 <https://doi.org/10.1111/1365-2656.12786>
- 770 Salathe, M., & Jones, J. H. (2010). Dynamics and Control of Diseases in Networks with Community
771 Structure. *PLoS Computational Biology*, 6(4). e1000736.
772 <https://doi.org/10.1371/journal.pcbi.1000736>
- 773 Seaholm, S. K., Ackerman, E., & Wu, S. (1988). Latin hypercube sampling and the sensitivity analysis of a
774 Monte Carlo epidemic model. *International Journal of Bio-Medical Computing*, 23(1-2), 97-112.
775 [https://doi.org/10.1016/0020-7101\(88\)90067-0](https://doi.org/10.1016/0020-7101(88)90067-0)
- 776 Silk, M. J., Croft, D. P., Delahay, R. J., Hodgson, D. J., Weber, N., Boots, M., & McDonald, R. A. (2017). The
777 application of statistical network models in disease research. *Methods in Ecology and Evolution*,
778 8(9), 1026–1041. <https://doi.org/10.1111/2041-210X.12770>
- 779 Springer, A., Kappeler, P. M., & Nunn, C. L. (2017). Dynamic vs. static social networks in models of
780 parasite transmission: predicting *Cryptosporidium* spread in wild lemurs. *Journal of Animal*
781 *Ecology*, 86(3), 419–433. <https://doi.org/10.1111/1365-2656.12617>
- 782 Stroeymeyt, N., Grasse, A. V., Crespi, A., Mersch, D. P., Cremer, S., & Keller, L. (2018). Social network
783 plasticity decreases disease transmission in a eusocial insect. *Science*, 362(6417), 941-945.
784 <https://doi.org/10.1126/science.aat4793>
- 785 Titcomb, E. M., O’Corry-Crowe, G., Hartel, E. F., & Mazzoil, M. S. (2015). Social communities and
786 spatiotemporal dynamics of association patterns in estuarine bottlenose dolphins. *Marine*
787 *Mammal Science*, 31(4), 1314–1337. <https://doi.org/10.1111/mms.12222>

788 Valsecchi, E., Amos, W., Raga, J. A., Podestà, M., & Sherwin, W. (2004). The effects of inbreeding on
789 mortality during a morbillivirus outbreak in the Mediterranean striped dolphin (*Stenella*
790 *coeruleoalba*). *Animal Conservation*, 7(2), 139–146. <https://doi.org/10.1017/S1367943004001325>

791 Van Bresseem, M. F., Van Waerebeek, K., & Raga, J. A. (1999). A review of virus infections of cataceans
792 and the potential impact of morbilliviruses, poxviruses and papillomaviruses on host population
793 dynamics. *Diseases of Aquatic Organisms*, 38(1), 53–65. <https://doi.org/10.3354/dao038053>

794 Van Bresseem, M. F., Raga, J. A., Di Guardo, G., Jepson, P. D., Duignan, P. J., Siebert, U., Barrett, T., Santos,
795 M. C. O., Moreno, I. B., Siciliano, S., Aguilar, A., & Van Waerebeek, K. (2009). Emerging infectious
796 diseases in cetaceans worldwide and the possible role of environmental stressors. *Diseases of*
797 *Aquatic Organisms*, 86, 143–157. <https://doi.org/10.3354/dao02101>

798 Van Bresseem, M. F., Duignan, P. J., Banyard, A., Barbieri, M., Colegrove, K. M., De Guise, S., Di Guardo,
799 G., Dobson, A., Domingo, M., Fauquier, D., Fernandez, A., Goldstein, T., Grenfell, B., Groch, K. R.,
800 Gulland, F. Jensen, B. A., Jepson, P. D., Hall, A., Kuiken, T., Mazzariol, S. Morris, S. E., Nielsen, O.,
801 Raga, J. A., Rowles, T. K., Saliki, J., Sierra, E., Stephens, N., Stone, B., Tomo, Ikuko, Wang, J.,
802 Waltzek, T., & Wellehan, J. F. X. (2014). Cetacean Morbillivirus: Current Knowledge and Future
803 Directions. *Viruses*, 6(12), 5145–5181. <https://doi.org/10.3390/v6125145>

804 Vaughan, K., Del Crew, J., Hermanson, G., Wloch, M. K., Riffenburgh, R. H., Smith, C. R., & Van Bonn, W.
805 G. (2007). A DNA vaccine against dolphin morbillivirus is immunogenic in bottlenose dolphins.
806 *Veterinary Immunology and Immunopathology*, 120(3–4), 260–266.
807 <https://doi.org/10.1016/j.vetimm.2007.06.036>

808 Wang, W., Tang, M., Zhang, H., Gao, H., Do, Younghae, & Liu, Z. (2014) Epidemic spreading on complex
809 networks with general degree and weight distributions. *Physical Review E*, 90, 042803.
810 <https://doi.org/10.1103/PhysRevE.90.042803>

811 Wierucka, K., Verborgh, P., Meade, R., Colmant, L., Gauffier, P., Esteban, R., de Stephanis, R., & Canadas,
812 A. (2014). Effects of a morbillivirus epizootic on long-finned pilot whales *Globicephala melas* in
813 Spanish Mediterranean waters. *Marine Ecology Progress Series*, 5021–10.
814 <https://doi.org/10.3354/meps10769>

815 Whitehead, H. (1995). Investigating structure and temporal scale in social organizations using identified
816 individuals. *Behavioral Ecology*, 6(2), 199–208.

817 Whitehead, H. (2008). *Analyzing Animal Societies: Quantitative Methods for Vertebrate Social Analysis*.
818 University of Chicago Press.

819 Wu, J., Dhingra, R., Gambhir, M., & Remais, J. V. Sensitivity analysis of infectious disease models:
820 methods, advances and their application. *Journal of the Royal Society Interface*, 10(86), 20121018
821 <https://dx.doi.org/10.1098%2Frsif.2012.1018>

822 Yange, Z., & Zhou, T. (2012). Epidemic Spreading in Weighted Networks: An Edge-Based Mean-Field
823 Solution. *Physical Review E* 85, 056106. <https://doi.org/10.1103/PhysRevE.85.056106>

824 Yee, T. W. (2018). VGAM: Vector Generalized Linear and Additive Models. R package version 1.0-5. URL
825 <https://CRAN.R-project.org/package=VGAM>

826

827

828

829

830

831

832

833

834

835

836 **Figure 1.** Respiratory contacts in the southern resident killer whale population. a) Example photographic
837 sequence of a successive surfacing between two individuals (J42 and J16). Individual J42 is identifiable
838 from her saddle patch in (i), and as J42 begins to submerge in (ii), individual J16 begins surfacing within
839 one body length. In (iii), J16 is fully identifiable. b) Final respiratory contact network for the population
840 from 2011 to 2015. Edge thickness corresponds to estimated daily probabilities of respiratory contact.
841 Node colors indicate pod membership (blue = J, green = K, orange = L) and dotted lines indicate clusters
842 found by walktrap community detection algorithm.

843

844 **Figure 2.** Distribution of disease outcomes in the observed network and two null models. Violin plots
845 indicate the density of disease outcomes (in proportion of the population infected). Dotted line indicates
846 our threshold for an unusual mortality event. Boxplots indicate quantiles for the runs in which the
847 epidemic resulted in a UME.

848

849 **Figure 3.** Results of simulated vaccination strategies. Lines indicate UME probability for each vaccination
850 strategy (solid = random, dashed = weighted degree, dotted = betweenness) under different levels of
851 coverage. Red dotted line indicates our conservative vaccination target, at which UMEs are predicted to
852 occur in less than 5% of cases.

853

854

855

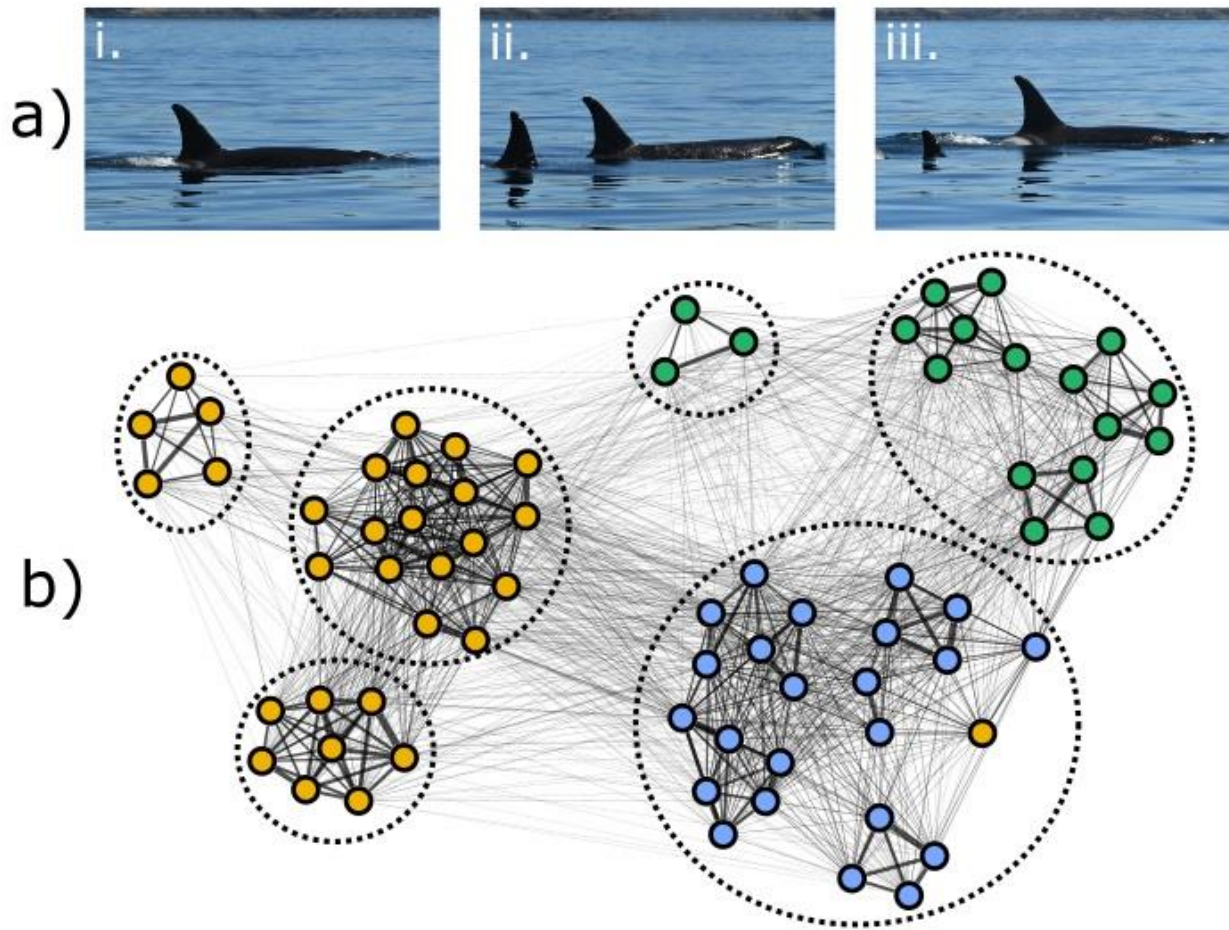
856

857

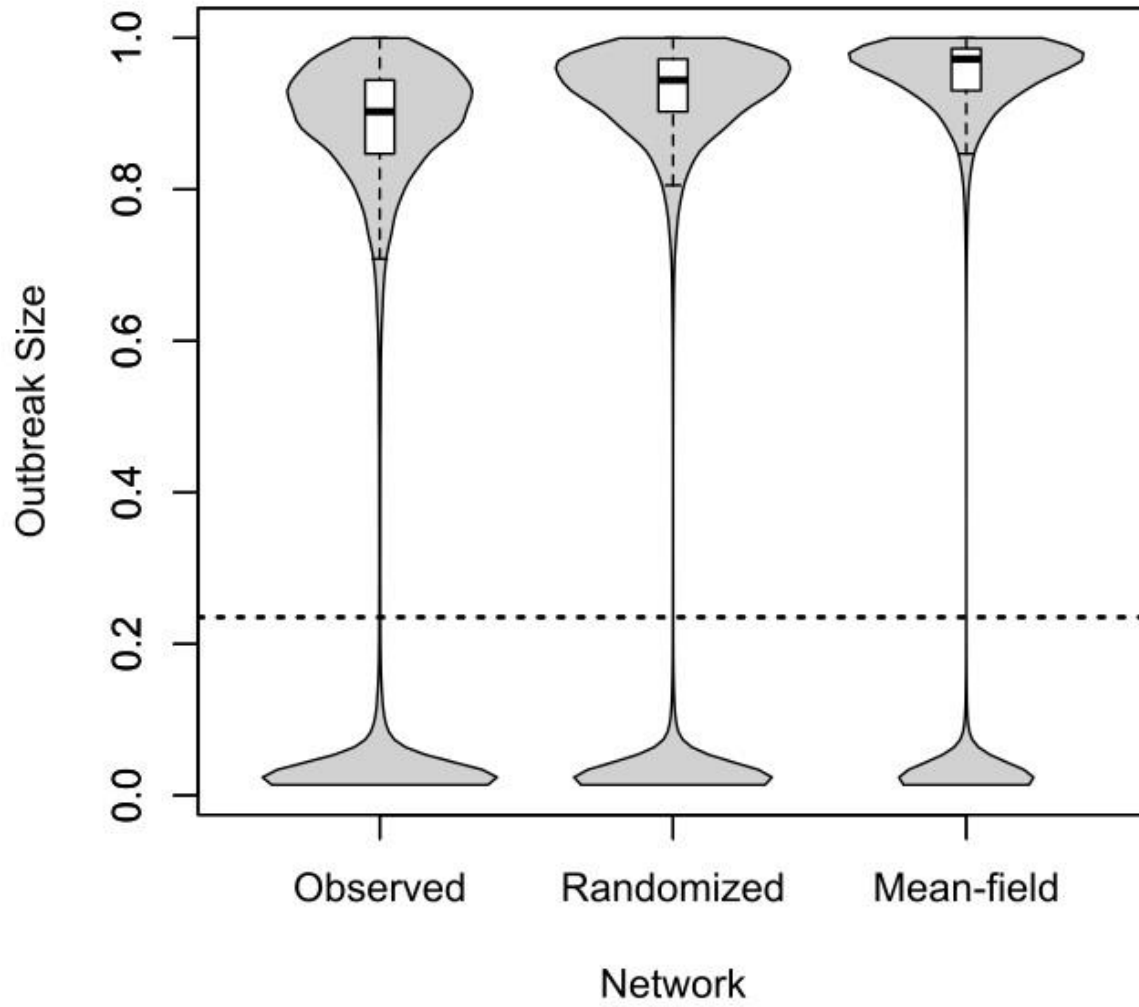
858

859

860 Figure 1.



861
862
863
864
865
866
867
868



870

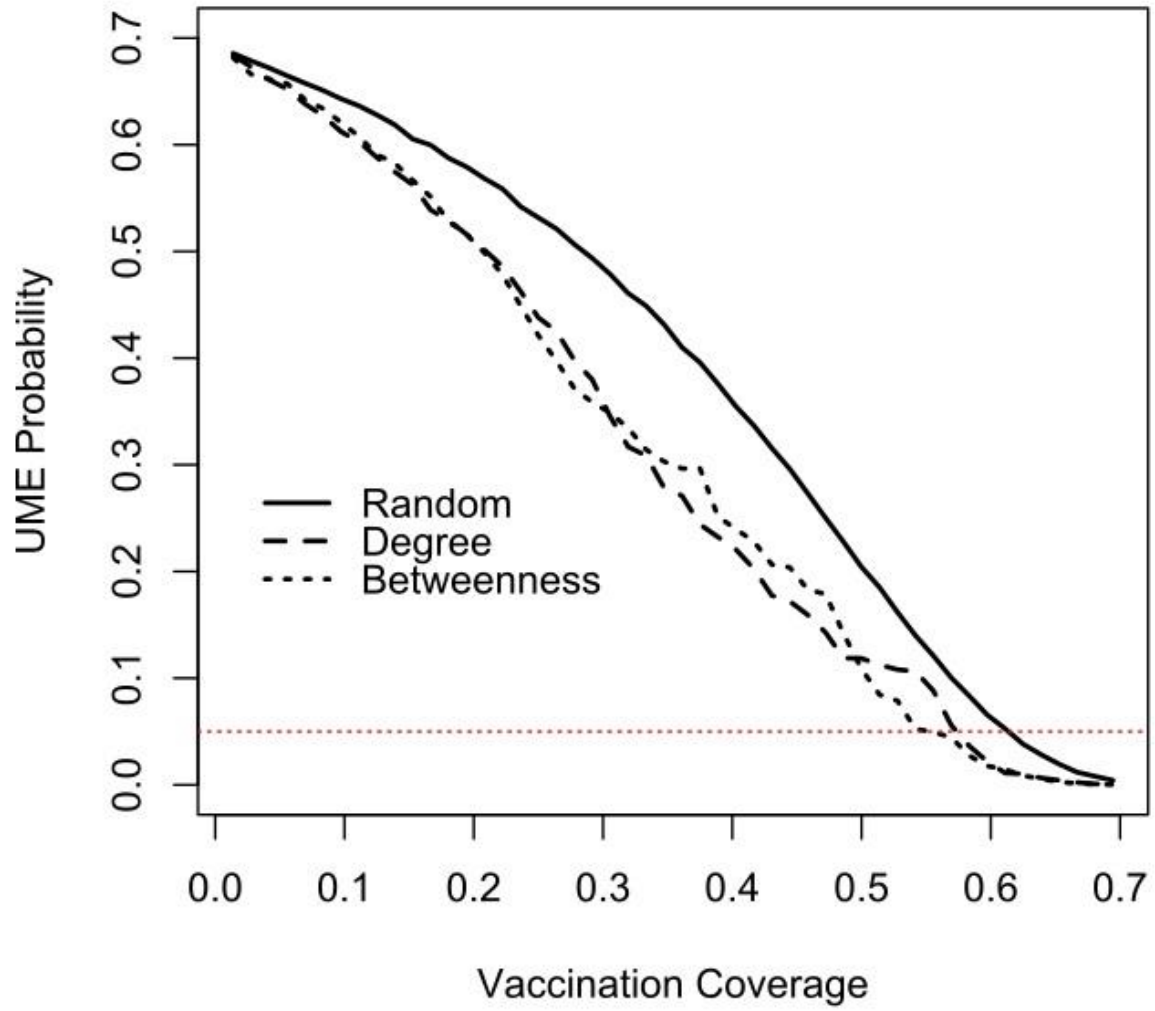
871

872

873

874

875 Figure 3.



876

877

878

879

880 **Table 1.** Parameters and values used for disease simulations. All parameter ranges were derived from
 881 studies of social interactions and CeMV epizootics in western Atlantic *T. truncatus*.

Parameter	Interpretation	Value	Source
α	Probability of removal per day	0.10 – 0.14	Morris <i>et al.</i> 2015
$1/\alpha$	Mean infectious period	7.14-10.00	Morris <i>et al.</i> 2015
R_0	Mean number of secondary cases per infected individual during an outbreak	2.08 – 3.17	Morris <i>et al.</i> 2015
$\langle s \rangle$	Mean number of contacts per individual per day	1.63 – 2.13	Titcomb <i>et al.</i> 2015
β	Per-contact transmission probability	$\frac{R_0\alpha}{\langle s \rangle}$	Kamp <i>et al.</i> 2013

882

883

884

885

886

887

888

889

890

891

892

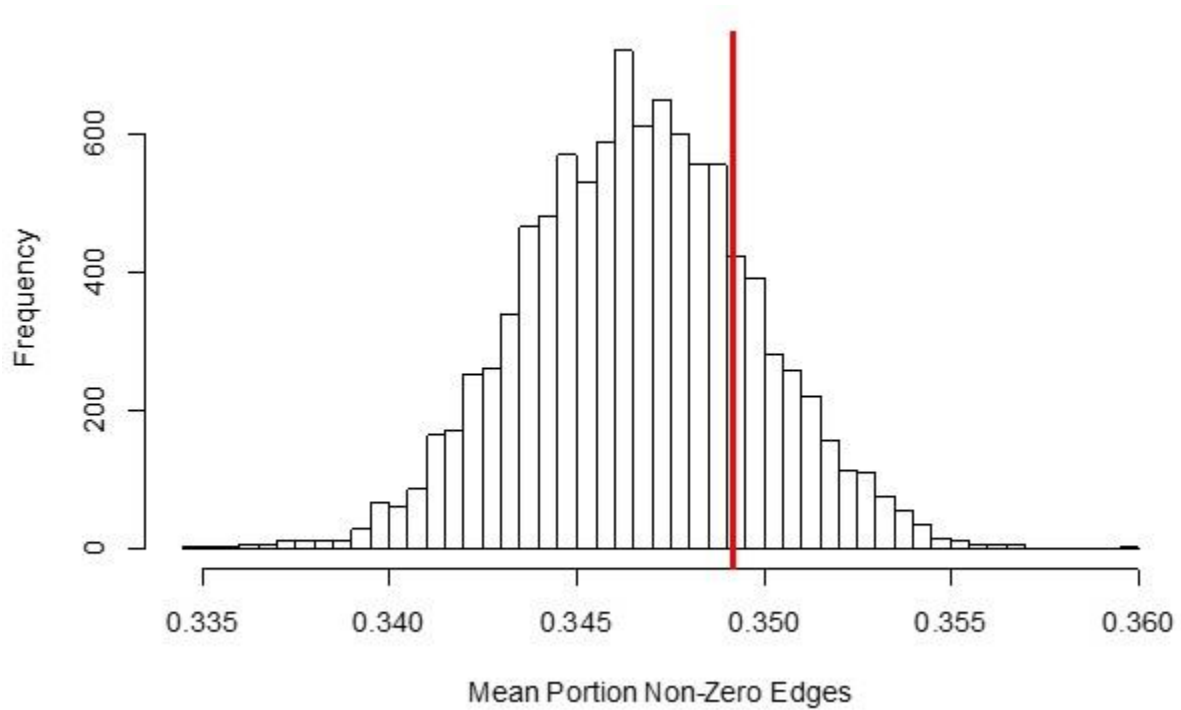
893

894

895

896 **Supplementary Figures**

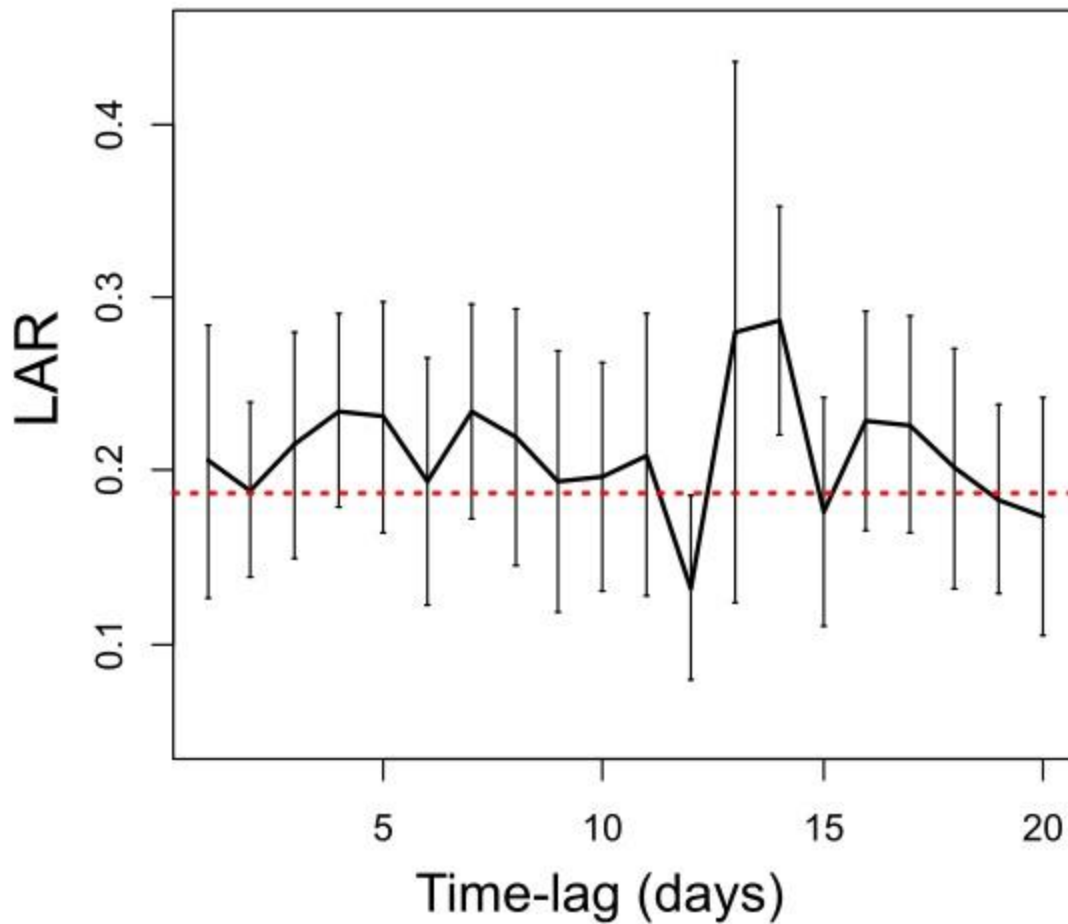
897



898

899 **Supplementary Figure 1.** Results of simulation comparing density of annual networks to aggregated
900 network. Histogram represents the mean density of annual networks simulated from the aggregated
901 contact probabilities and yearly dyadic sampling effort. Red line indicates the observed mean density of
902 annual networks.

903



904

905 **Supplementary Figure 2.** Lagged association rates of respiratory contacts. Black line is the calculated LAR
 906 at each daily time-lag, with error bars indicating jackknifed 95% confidence intervals. Dotted red line
 907 indicates the expected LAR under temporal independence, given the observed association preferences
 908 (as in equation 2).